Femtosecond excitation cavity studies and superluminescence by two-photon absorption in vertical cavity lasers at 300 K

R. Schroeder,[1,][*]A. Knigge,[2] M. Zorn,[2] M. Weyers,[2] and B. Ullrich[1]

[1]*Centers for Materials Science and Photochemical Sciences, Department of Physics and Astronomy, Bowling Green State University, Bowling Green, Ohio 43403-2204*

[2]*Ferdinand-Braun-Institut für Höchstfrequenztechnik, Albert-Einstein-Strasse 11, D-12489 Berlin, Germany*

Vertical cavity semiconductor lasers have become the main instrument in the application field of inexpensive, low to midrange power, and high-efficiency lasers. Electrical as well as electroluminescence properties of these lasers can readily be examined. However, for an investigation of the bulk, and most importantly, the active zone, the majority of conventional optical methods fail due to the high reflectivity of the cavity mirrors or the absorption of the excitation beam by the mirror material. Laser pulses as short as 200 fs at 804 nm have been applied to invoke two-photon excited photoluminescence and superluminescence of a vertical cavity surface-emitting laser based on a $Ga_xIn_{1-x}P$ core at room temperature. From the analysis of the emission and laser spectra, important properties are found, such as the redshift of the emission wavelength due to many-body effects, which was confirmed by analysis of the cavity without mirrors.

I. INTRODUCTION

Vertical cavity surface-emitting laser (VCSEL) structures are of increasing importance in the semiconductor laser field because they offer large advantages over edge-emitting lasers such as the ease of two-dimensional structured fabrication, circular beam profiles, and dynamic single-frequency operation.[1–5] Although they are already commonly used for infrared emitting laser applications, the move to visible wavelengths is difficult and has led to strong research efforts in the past years. A promising emitting material for visible red laser emission, such as that used for digital versatile discs (DVD's) is $Ga_xIn_{1-x}P$, which has been studied in detail.[6–12] There are several important properties to be controlled: The reversed band offsets of the sandwiched distributed Bragg reflectors (DBR's) and the optical cavity material and an optimized doping profile are the big challenges from an electronic point of view; the lattice mismatch and the $AlAs/Al_xGa_{1-x}As$ interfaces are challenges from a crystallographic point of view.[12]

An important step to master the formation of VCSEL structures is the tight control over the manufacturing processes. With common methods, it is difficult to distinguish advancements in electronic conductivity from better optoelectronic properties leading to higher emission efficiencies. Regular photon spectroscopy has to deal with strong absorption in the DBR and the laser cavity and does not allow sampling of the active layer directly. By means of photomodulated reflectance studies, however, VCSEL's have been studied nondestructively in the past, as well.[13,14] Our trials of probing the VCSEL structures studied here with laser excitation at 632 and 532 nm did not show any photoluminescence.

In this paper, we propose the use of two-photon excitation to quantitatively measure the bulk properties without the influence of electrical properties inherent to a specific production method. The excitation at 804 nm (1.54 eV) is well out of the absorption range of the investigated VCSEL, which is formed by a $Ga_xIn_{1-x}P$ active layer quantum well, $Al_xGa_yIn_{1-x-y}P$ cavity spacers, and $AlAs/Al_xGa_{1-x}As$ Bragg mirrors. Two-photon absorption is well suited for measurements penetrating deep into a layer structure of a sample since the absorption coefficients are smaller and also because the decay of the intensity is not exponential, but varies with reciprocal length. Additionally, since the DBR's were tuned to reflect around the VCSEL emission wavelength, the lower-energy excitation laser pulses were able to excite the whole sample. The important difference between single-photon and two-photon excitation is that although for both the DBR's are reflective and absorptive, only the two-photon excitation can penetrate the DBR's effectively enough to excite the active zone significantly.

The two-photon excitation was generated by an ultrafast laser system. As such the excitation is a purely coherent two-photon excitation, which means that two photons are absorbed by one electron at once, and the final state has an even parity to the initial state.

II. EXPERIMENT

Three different VCSEL structures were analyzed using two-photon absorption. One VCSEL structure [Fig. 1(a), left] was a microcavity light-emitting device (LED), i.e., a mini-VCSEL structure, which only features line narrowing. However, due to the smaller number of DBR's, 15.5 pairs on the back-reflector side and 7 pairs on the emission side, not only the main emission of the GaInP active layer could be probed but also characteristic signatures of elements of the cavity and mirrors were sampled. The other two structures [Fig. 1(a), right] have identical numbers of DBR's, 55.5 pairs on the back side and 35 on the emission side, but the cavities are optimized for different wavelengths due to different optical lengths of the cavities. The microcavity LED will be referred
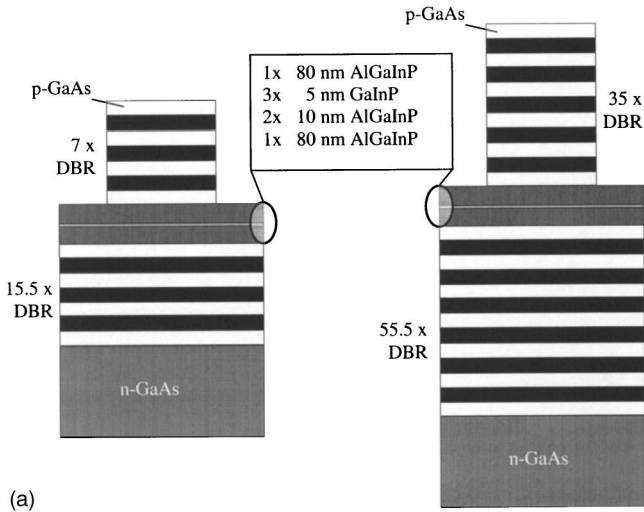
(a)
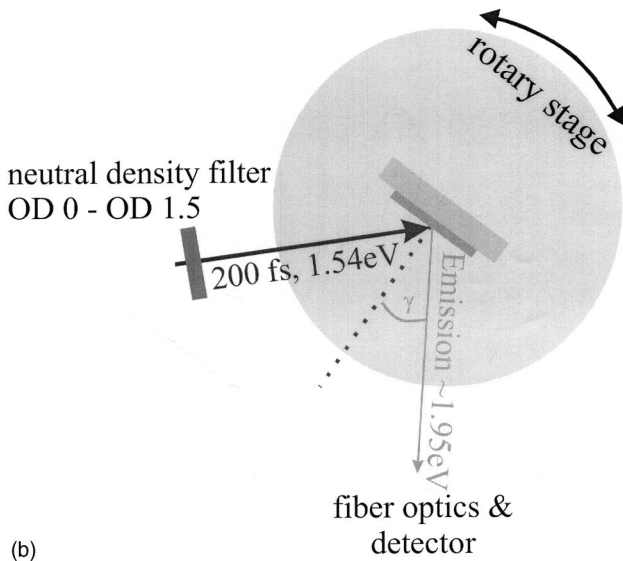
(b)

FIG. 1. (a) VCSEL structures with GaInP as the active layer, $Al_xGa_yIn_{1-x-y}P$ as the cavity spacers, and $AlAs/Al_xGa_{1-x}As$ as Bragg mirrors. Left side, microcavity LED (referred to as VCSEL 2 in the text); right side, regular VCSEL structures (referred to as VCSEL 1 and 3 in the text). The difference between VCSEL 1 and 3 lies solely in a slightly altered cavity. (b) The measurement geometry for the luminescence experiments.

to as VCSEL 2 and the other two as VCSEL 1 and 3.

The formation of the VCSEL cells is described elsewhere.[12] The layered structures are shown in Fig. 1(a). The DBR's consist of alternating $Al_xGa_{1-x}As$ and AlAs layers. The n DBR's are Si doped, the p DBR's are C doped. The $Al_xGa_yIn_{1-x-y}P$ layers in the cavity adjacent to the DBR's are Si and C doped, as well. The samples were excited with a femtosecond laser system, a Coherent Innova Ar^+ laser powering a Coherent Mira Ti:sapphire oscillator and a Coherent RegA amplifier. The incident laser beam was focused to less than 60 μm in radius. The laser beam has an energy of 2.8 μJ per pulse, a repetition rate of 249 kHz, and a pulse width of approximately 200 fs. Thus, the maximum excitation intensity is 180 GW cm^{-2}. The photon energy of

the laser is 1.54 eV (804 nm). The photoluminescence of the sample was detected with a 100-μm fiber, which is transmissive in the visible and ultraviolet spectral range, and an attached fiber optics spectrometer. The measurement geometry is shown in Fig. 1(b). Owing to the high reflectivity of the DBR array on the substrate, and the fact the GaAs substrate is highly absorptive in the whole visible region, the active layer emission had to be detected through the less-reflective top DBR array. Since the fiber could not be placed in the excitation beam, the sample was tilted several degrees with respect to the incident laser beam. All experiments were performed at room temperature. The angle of incidence was kept at 30°; the detector angle γ was optimized for the strongest emission of the sample. For the intensity-dependent measurements, the laser excitation was attenuated using neutral-density filters that were previously calibrated for power throughput.

III. DISCUSSION

Except for the GaAs layers [as seen in Fig. 1(a), bottom and top] the whole VCSEL structure does not show single-photon absorption for the 1.54-eV laser beam. For two-photon absorption, the change in intensity per space element is

$$\frac{dI}{dx} = -\alpha_2 I^2, \tag{1}$$

where I is the intensity and α_2 is the two-photon absorption coefficient. Integration over the whole thickness leads to the well-known equation

$$\frac{1}{T} = \alpha_2 I_0 t + 1, \tag{2}$$

where T is the transmission, I_0 is the incident intensity, and t is the thickness. It has to be noted that Eq. (2) only holds for constant α_2, an assumption valid for the intensities used to probe the VCSEL structure presented.

The generated electron-hole pairs per laser pulse are expressed by

$$G_{pulse} = \frac{E_{pulse}(1-T)}{2E_{photon}V}, \tag{3}$$

where E_{pulse} is the energy per pulse, E_{photon} is the energy per single photon, and V is the excited volume. Inserting Eq. (2) into Eq. (3) and substituting $E_{pulse} = I_0 \tau_{pulse} A_{beam}$ leads to

$$n_{pulse} = G_{pulse} = \frac{\tau_{pulse} A_{beam}}{2E_{photon}V} \frac{I_0^2 \alpha_2 t}{I_0 \alpha_2 t + 1}, \tag{4}$$

where n_{pulse} is the number of electron-hole pairs created, τ_{pulse} is the laser pulse duration, and A_{beam} is the area of the laser beam. For $I_0\alpha_2 t \ll 1$, the generation term has a quadratic dependence on the incident intensity, which will be the case for the very thin films in the VCSEL structure. For thicker films or higher excitation intensity, the dependence will be subquadratic and finally linear for $I_0\alpha_2 t \gg 1$. At the maximum intensity value $I_0 = 180$ GW/cm^2, we get $I_0\alpha_2 t$
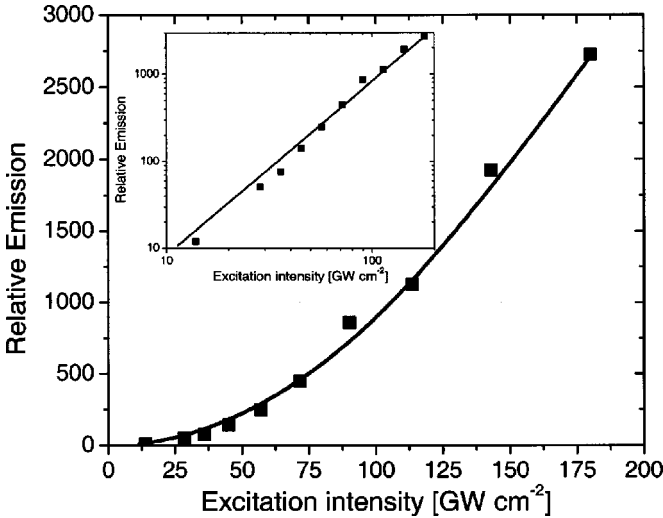
FIG. 2. Maximum of the emission intensity of the VCSEL 2 vs excitation intensity. The measured intensities are depicted as full squares; a theoretical quadratic dependence is shown as solid line. The emission is dependent on the squared incident intensity, as is characteristic for two-photon excitation. The inset shows the same graph in a double-logarithmic scale.

FIG. 3. From left to right: Normalized two-photon excited peak emission of VCSEL 1, 2, and 3 at low (L) intensities (≈ 10 GW cm^{-2}) and high (H) intensities (≈ 180 GW cm^{-2}). The VCSEL 2 emission spectra do not show superluminescence since there are only 15.5 and 7 mirror pairs providing the feedback. VCSEL 1 and 3 with 35 and 55.5 mirror pairs show two-photon induced superluminescence. The wavelength scale on the bottom x axis is linear; the energy scale on the top x axis is reciprocal. The inset shows the shift in wavelength for VCSEL 1 at two different angles, but constant intensity. The emission peaks at 55° and 60° match the high- and low-intensity spectra depicted as curves 1L and 1H exactly.

$= 0.005 \ll 1$, using the literature value of $\alpha_2 = 9$ cm/GW for InP (Ref. 15) and an active layer thickness of $t \approx 20$ nm. Hence, with Eq. (4) it is possible to check the regime of the measurement.

Figure 2 shows the dependence of the emission from the Ga$_x$In$_{1-x}$P active layer with respect to the incident laser intensity. The measured points and the theoretical quadratic dependence curve lie on top of each other. The perfect quadratic dependence and the fact that there are 4 μs between two pulses are strong evidence for coherent two-photon excitation in the regime of $I_0 \alpha_2 t \ll 1$. Since the dependence of the photoluminescence on the incident intensity in Fig. 2 is exactly quadratic, it follows that the photoluminescence depends linearly upon the number of excited species, which in turn depends in a quadratic manner on the intensity (two-photon absorption). This may seem surprising for carrier densities as high as 10^{19} cm^{-3}, but due to the high reflectivity of the DBR's, photons can induce many carrier recombinations.

Additionally, Eq. (4) allows the estimation of n_{pulse} for the active Ga$_x$In$_{1-x}$P layer. We did not find a α_2 value for Ga$_x$In$_{1-x}$P in the literature; however, the two-photon absorption coefficient for InP of 9 cm/GW (Ref. 15) is a good approximation. The top GaAs cladding layer both reflects and absorbs the incident laser beam. The intensity behind the cladding layer is $\approx 70\%$ of the incident beam. The reflection was measured to be on the order of 20%, and the absorption of the layer was estimated. With $V = A_{\text{beam}} t$, $E_{\text{photon}} = 1.54$ eV, $I_0 = 180 \times 0.7$ GW cm^{-2}, and $I_0 \alpha_2 t \ll 1$, it follows that $n \approx 10^{19}$ cm^{-3}. This is the number of charge carriers directly after the absorption, which takes place in 200 fs. Since the stimulated emission takes place in the picosecond range, the "effective" number of charge carriers is 1–2 orders of magnitude lower.

In Fig. 3 the emission peaks of the Ga$_x$In$_{1-x}$P active layers of the VCSEL 1,2,3 structures are shown. The full width at half maximum (FWHM) is 20 meV (6.5 nm), linenarrowed stimulated emission, for VCSEL 2, the microcavity LED with a low number of mirror pairs. The FWHM is only 5 meV (1.8 nm) for VCSEL 1 and 3. The reason for the appearance of superluminescence for VCSEL 1 and 3 is the more than tripled number of DBR mirror pairs. The label H denotes a high excitation density of 170–180 GW cm^{-2}; the label L denotes a lower excitation density of 10–15 GW cm^{-2}. It is apparent that all three samples show a shift of the peak luminescence as a function of the intensity; the shift appears to be very similar in all three cases.

Figure 4 shows the underlying mathematical proportionality of the relative peak positions for the samples for several different incident intensities. The shift in energy is proportional to the intensity and is directly related to a change in the absorption gap of the emissive material. This phenomenon is caused by optically induced band-gap narrowing as observed recently in thin-film CdS under comparable experimental conditions.[16]

Band-gap narrowing is a many-body effect due to the Fermi repulsion of electrons. In general,[17] band-gap shrinkage is described with the equation below:

$$\Delta E_g = -k n^{1/d}, \tag{5}$$
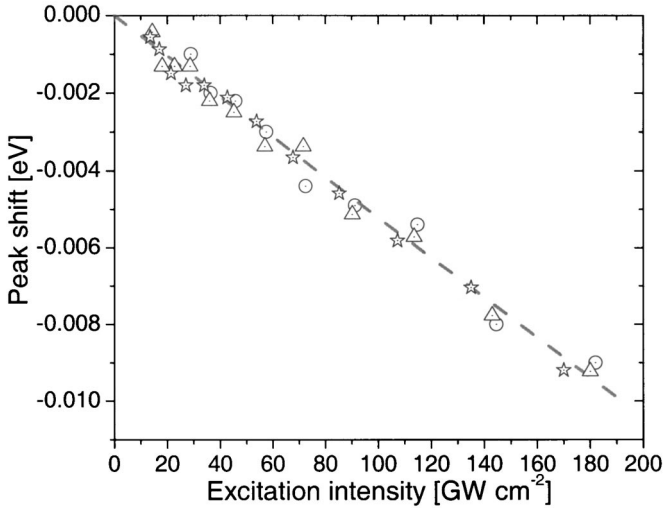
FIG. 4. Emission peak shifts vs incident intensity for VCSEL 1 (stars), VCSEL 2 (circles), and VCSEL 3 (triangles). A linear fit describes the band-gap narrowing very well for all three samples.

where ΔE_g is the lowering of the band-gap energy, n is the number of charge carriers, d is the exponent, which can vary from 2 to 6, and k is a proportionality factor. Using Eq. (4) in the $I_0\alpha_2 t \ll 1$ regime and with $V = A_{\mathrm{beam}}t$, it follows from Eq. (5)

$$\Delta E_g = -k\left(\frac{\tau_{\mathrm{pulse}}\alpha_2}{2E_{\mathrm{photon}}}\right)^{1/d} I_0^{2/d}. \qquad (6)$$

Figure 4 follows the model very closely and the exponent is found to be $d=2$. The proportionality factor between ΔE_g and I_0 is found via linear regression to be $b = -5.2 \times 10^{-5}$ eV cm^2/GW, and after correcting for reflection and absorption losses of about 30%, $b = -7.4 \times 10^{-5}$ eV cm^2/GW (note that $d=2$):

$$b = -k\sqrt{\frac{\tau_{\mathrm{pulse}}\alpha_2}{2E_{\mathrm{photon}}}}. \qquad (7)$$

From Eq. (7) k can be estimated: $k \approx 3 \times 10^{-34}$ J m$^{3/2}$. Since the dimensionality of n was found to be $d=2$, which corresponds to the case of band-gap narrowing due to the Coulombic interaction (Debye model), it would be interesting to compare k to the value for the Debye model. The active layer is a quantum well; therefore the Debye model oversimplifies the problem. The proportionality factor is[17]

$$k = \frac{q^3}{4\pi(\varepsilon\varepsilon_0)^{3/2}\sqrt{k_B T_c}}, \qquad (8)$$

where q is the electron charge, k_B is Boltzmann's constant, T_c is the temperature of the charge carriers, ε_0 is the dielectric constant, and ε is the dielectric permittivity of the layer. The dielectric permittivity for $Ga_x In_{1-x}P$ is 12 (Ref. 18), and $k_B T_c$ was assumed to be ≥ 25 meV (room temperature); charge-carrier temperatures are typically higher than lattice temperatures, and thus the value given in Eq. (8) is the lower
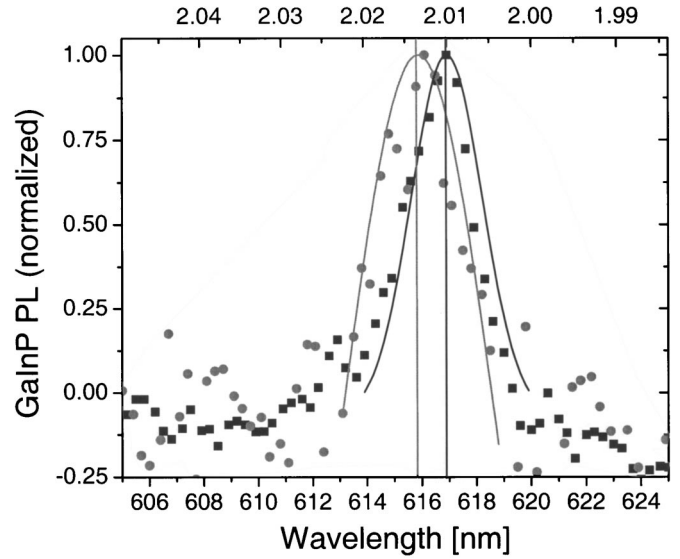
FIG. 5. Photoluminescence spectra of an Al-Ga-In-P/$Ga_x In_{1-x}P$ cavity without mirrors. The right curve has been measured with an incident intensity of 215 GW cm^{-2}, the left curve with 54 GW cm^{-2}. The data points have been fitted with a Gaussian theoretical curve to determine the peak position more accurately.

limit. Charge-carrier temperatures are often found to be 370–480 K, or $k_B T_c = 30$–40 meV.[15,19]

From Eq. (8), the proportionality factor is calculated to $k \approx 10^{-33}$ J m$^{3/2}$. This is not a perfect agreement with the value obtained from the experiment and Eq. (7), and therefore the Debye model is indeed too simple to describe the band-gap narrowing satisfying in the VCSEL. It is, however, a useful approximation.

It has been pointed out in Ref. 20 that a similar effect of redshifting can occur due to temperature elongation of the cavity. However, in this case the average intensity per second (i.e., cw intensity) is not high enough to heat the sample by several ten degrees Celsius, which would be the necessary value for the observed redshift. Also, as has been noted above, the cavities of the investigated VCSEL's are tuned for different wavelengths, yet the relative shift stays constant. This is very strong evidence that the band-gap shrinkage of the VCSEL's does not depend on specific cavity features.

To verify whether or not band-gap shrinkage really occurs, or if the effect is due to thermal expansion and/or changes in the refractive index, we repeated the measurements for a different device without the DBR's. The structure of this cavity is identical to that of the previously discussed VCSEL structures, but without the addition of the top and bottom DBR's. This means that the cavity is in direct contact with the GaAs substrate.

Upon evaluation of the photoluminescence, depicted in Fig. 5, two details become apparent: There is a shift to lower energies for higher intensities, albeit smaller, and the emission is very weak compared to the VCSEL structures. This leads to believe that the presence of the lower-band-gap material GaAs significantly reduces the number of electron-hole pairs in the cavity when not interfaced with several hundred nanometers of DBR's. Judging from the intensity of the
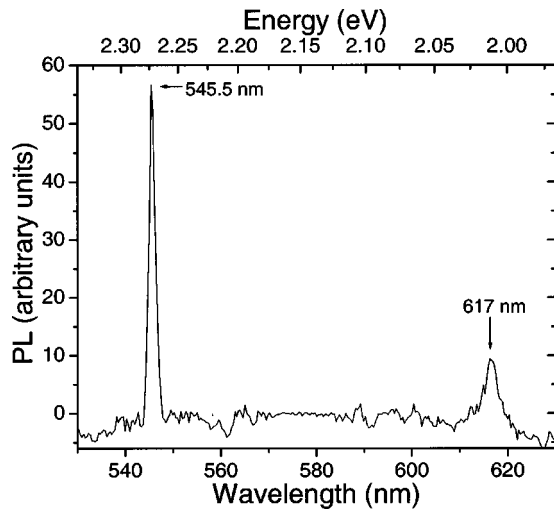
FIG. 6. Two-photon excited emission peaks of cavity and DBR's in VCSEL 2. The left peaks at 545.5 and 617.0 nm stem from $Al_{0.25}Ga_{0.25}In_{0.5}P$ and $Al_{0.5}Ga_{0.5}As$, respectively. The wavelength scale on the bottom x axis is linear; the energy scale on the top x axis is reciprocal.

emission, a decrease of at least one order of magnitude in the number of electron-hole pairs is expected. The shift observed in Fig. 5 is about 3 meV, which is expected when analyzing Fig. 4 for low intensities.

Although the emission wavelength of the active $Ga_xIn_{1-x}P$ layers in the VCSEL is determined in part by the DBR's, it is also modified by the cavity gain curve, the actual emission wavelength being the convolution of the two.[21] It is exactly the cavity gain curve that is altered by the band-gap shrinkage, as it can be observed for the emission of just the cavity without the DBR's as well. While the high number of DBR's in the VCSEL structures selects the wavelength very narrowly, i.e., $\Delta\lambda < 1$ nm, the resonance wavelength strongly depends on the measurement angle. It can be seen from the inset in Fig. 3 that the angles for the high-intensity emission and the low-intensity emission for VCSEL 2 (cf. Fig. 3) are just separated by 5°. Since we measured close to the surface, the detection fiber could easily pick up both angles at once.

It is important to note that this band-gap narrowing not only occurs for optical pumping, as in this case, but also due to electrical pumping. Therefore, it is important to keep this shift in mind when designing the VCSEL for the desired emission wavelength.

Apart from $Ga_xIn_{1-x}P$ emission from the active quantum wells, emission features from cavity spacer and DBR mirror materials were also measured. The emission peaks are de-picted in Fig. 6. It is important to determine the peak luminescence position of both, as they are indicators for the actual band gap of the outer materials; it is imperative that the band-gap energies of all outer materials are substantially higher than the highest energy of the cavity gain curve.

The two emission peaks are located at 546 nm (2.27 eV) and 617 nm (2.01 eV), respectively. From Refs. 22 and 23 the peaks can be assigned to the outer materials. For $Al_xGa_{0.5-x}In_{0.5}P$, the band-gap energy is reported as 2.30–2.33 for $x=0.25$. This corresponds to the emission peak at 2.27 eV. For $Al_xGa_{1-x}As$, the reported values are $E_g = 1.705 + 0.695x$ for the X conduction-band minimum, which is the lowest for $x > 0.47$. For the VCSEL structures discussed in this paper, $x = 0.5$, and $E_g = 2.053$ eV (or 604 nm), which is in reasonable agreement with the photoluminescence peak of 2.01 eV. As such, the respective band-gap energies for $Al_{0.25}Ga_{0.25}In_{0.5}P$ and $Al_{0.5}Ga_{0.5}As$ have been determined to be at a reasonable distance from the highest observed emission energy of GaInP in VCSEL 1, $E_{photon} = 1.96$ eV, or 632.5 nm.

IV. CONCLUSIONS

We report probing of the active zone of VCSEL structures using two-photon excitation with 200-fs pulses at 1.54 eV at room temperature. This excitation in the femtosecond regime causes superluminescence in the VCSEL structures 1 and 3 that feature 55.5 and 35 mirror pairs and line-narrowed emission in the microcavity LED (VCSEL 2) with 15.5 and 7 mirror pairs. Optically induced band-gap shrinkage due to many-body effects in the $Ga_xIn_{1-x}P$ active layer was measured for all samples showing almost identical behavior. The band-gap shrinkage was determined to have a square-root dependence on the number of optically induced charge carriers. The proportionality factor was found to be similar to that of the Debye model. The value for the band-gap shrinkage is important knowledge for the design of the VCSEL cavity, as it can occur both under optical and electrical excitation. Additionally, by measuring the emission peaks of the mirror materials, the actual optical band gap of the mirrors is found and is a useful value to determine the degree of optimization of the different layers for the desired VCSEL application. We show that with two-photon excitation, the cavity of a VCSEL can be probed, without damage to the sample.

ACKNOWLEDGMENT

*Electronic address: raoul@kottan-labs.bgsu.edu

[1] R. F. M. Hendricks, M. P. van Exter, J. P. Woerdman, A. van Geelen, L. Weegels, K. H. Gulden, and M. Moser, Appl. Phys. Lett. **71**, 2599 (1997).

[2] D. Burak, S. A. Kemme, R. K. Kostuk, and R. Binder, Appl. Phys. Lett. **73**, 3501 (1998).

[3] S. J. Sweeney, G. Knowles, and T. E. Sale, Appl. Phys. Lett. **78**, 865 (2001).

[4] D. K. Serkland, K. D. Choquette, G. R. Hadley, K. M. Geib, and A. A. Allerman, Appl. Phys. Lett. **75**, 3754 (1999).

[5] J. M. Redwing, D. A. S. Loeber, N. G. Anderson, M. A. Tischler, and J. S. Flynn, Appl. Phys. Lett. **69**, 1 (1996).

[6] B. Pezeshki, M. Hagberg, M. Zelinski, S. D. DeMars, E. Kolev, and R. J. Lang, IEEE Photonics Technol. Lett. **11**, 791 (1999).

[7] O. Imafuji, T. Fukuhisa, M. Yuri, M. Manno, A. Yoshikawa, and K. Itoh, IEEE J. Sel. Top. Quantum Electron. **5**, 721 (1999).

[8] M. Kondow and S. Minagawa, J. Appl. Phys. **64**, 793 (1988).

[9] M. Guina, J. Dekker, A. Tukainen, S. Orsila, M. Saarinen, M. Dumitrescu, P. Sipalä, P. Savolainen, and M. Pessa, J. Appl. Phys. **89**, 1151 (2001).

[10] A. Oster, M. Zorn, K. Vogel, J. Fricke, J. Sebastian, W. John, M. Weyers, and G. Tränkle, in *Vertical-Cavity Surface-Emitting Lasers V*, edited by Kent Choquette and Chun Lei Proc. SPIE **4286**, 148 (2001).

[11] A. Knigge, M. Zorn, H. Wenzel, M. Weyers, and G. Tränkle, Electron. Lett. **37**, 1222 (2001).

[12] A. Bhattacharya, M. Zorn, A. Oster, M. Nasarek, H. Wenzel, J. Sebastian, M. Weyers, and G. Tränkle, J. Cryst. Growth **221**, 663 (2000).

[13] P. J. Klar, G. Rowland, P. J. S. Thomas, A. Onischenko, T. E. Sale, and T. J. C. Hosea, Phys. Rev. B **59**, 2894 (1999).

[14] T. J. C. Hosea, T. E. Sale, and P. J. S. Thomas, IEEE Photonics Technol. Lett. **12**, 1328 (2000).

[15] M. D. Dvorak, B. L. Justus, D. K. Gaskill, and D. G. Hendershot, Appl. Phys. Lett. **66**, 804 (1995).

[16] B. Ullrich and R. Schroeder, Semicond. Sci. Technol. **16**, L37 (2001).

[17] E. F. Schubert, Press Syndicate of the University of Cambridge, Cambridge, U.K. (1993).

[18] M. Bleicher, *Halbleiter-Optoelektronik*, (Dr. Alfred Hüthig Verlag, Heidelberg, Germany, 1986).

[19] P. Y. Yu and B. Welber, Solid State Commun. **25**, 209 (1978).

[20] V. Vilokkinen, P. Sipilä, P. Melanen, M. Saarinen, S. Orsila, M. Dumitrescu, P. Savolainen, M. Toivonen, and M. Pessa, Mater. Sci. Eng., B **74**, 165 (2000).

[21] *Vertical-Cavity Surface-Emitting Lasers*, edited by C. Wilmsen, H. Temkin, and L. A. Coldren (Cambridge University Press, Cambridge, U.K., 1999), pp. 198–200.

[22] X. H. Zhang, S. J. Chua, and W. J. Fan, Appl. Phys. Lett. **73**, 1098 (1998).

[23] *Data in Science and Technology: Semiconductors, Group IV Elements and III-V Compounds*, edited by O. Madelung (Springer, Heidelberg, Germany, 1991).